



Experimental and Numerical Investigations of Mechanical Behaviour for Titanium Bolted Joints with Friction Shim

Guillaume Pichon, Alain Daidié, Éric Paroissien, Audrey Benaben, Clément Chirol

► To cite this version:

Guillaume Pichon, Alain Daidié, Éric Paroissien, Audrey Benaben, Clément Chirol. Experimental and Numerical Investigations of Mechanical Behaviour for Titanium Bolted Joints with Friction Shim. International Joint Conference on Mechanics, Design Engineering & Advanced Manufacturing, Jun 2022, Ischia, Italy. pp.827-838, 10.1007/978-3-031-15928-2_72 . hal-03888060

HAL Id: hal-03888060

<https://hal.science/hal-03888060>

Submitted on 7 Dec 2022

HAL is a multi-disciplinary open access archive for the deposit and dissemination of scientific research documents, whether they are published or not. The documents may come from teaching and research institutions in France or abroad, or from public or private research centers.

L'archive ouverte pluridisciplinaire **HAL**, est destinée au dépôt et à la diffusion de documents scientifiques de niveau recherche, publiés ou non, émanant des établissements d'enseignement et de recherche français ou étrangers, des laboratoires publics ou privés.

Experimental and Numerical Investigations of Mechanical Behaviour for Titanium Bolted Joints with Friction Shim

Guillaume Pichon^{1, 2}, Alain Daidié¹[0000-0002-1772-9119], Éric Paroissien¹[0000-0002-8466-9419], Audrey Benaben² and Clément Chirol²

¹ Institut Clément Ader (ICA), Université de Toulouse, INSA, IMT MINES ALBI, ISAE-SUPAERO, UT III, Toulouse, France

² AIRBUS Operations S.A.S., Toulouse, France

Abstract. The work presented here is an experimental and numerical study on a new technology called friction shims. Those are thin shim made of steel with a shape of washer. Their coating made of nickel and micro diamonds aim to increase the friction coefficient when located at the interface of two parts. The mechanical behaviour as well as the static and fatigue strengths of titanium bolted joints with this specific technology are presented in this study. Specimens are representative of hole-to-hole aeronautical joints, involving large clearance and misalignments. Specimen geometrical and material definition are presented as well as test set up. The experimental test results show limited impact on the static strength and a large increase in the fatigue strength. A numerical analysis based on the finite element method was developed and correlated with the experiments to provides complementary information and to understand the mechanical behaviour observed during the static tests and the gain in fatigue strength.

Keywords: Hole-to-hole, Fatigue, Static, Testing, Finite Element Analysis.

1 Introduction

One of the main concerns of aircraft manufacturers is to be integrated into industry 4.0, for better agility in both design and manufacturing. This transition is achievable by the re-engineering of processes. This paper is set in the framework of the “hole to hole” bolted assembly process introduced by Bloem [1]. This process constitutes a great opportunity to revolutionize aeronautic assembly lines by having structural parts individually drilled before the assembly phase. However, the main consequence of this process is the potential for misalignments of bolt holes when parts are mated, making the bolt installation impossible. The solution proposed by Bloem [1] is to slightly increase the diameter of bolt holes so that assembly remains feasible.

The investigations on bolt hole clearance and error locations have been the subject of many publications, in particular concerning composite laminates [2-6]. According to these latest publications, clearance and misalignments have a significant effect on static and fatigue strengths. Such defects also have an impact on the loading behaviour, in

particular on the macro slipping, i.e. the slipping occurring at a joint interface when the shanks of the bolts and the holes of the plates are not in direct contact due to clearance. This macro slipping is an unwanted phenomenon. It is not present in current aeronautical joints due to fit clearance but it is inherent in hole-to-hole assembly. To delay this phenomenon, friction load at the joint interface is the best leverage to work on.

There are two ways to increase friction load at the interface. The first one is to increase the normal load, i.e. increase bolt loads. Several studies have investigated the effect of increasing bolt loads on the static and fatigue strengths [7-8] experimentally and numerically. Those works have shown a positive impact of increasing bolt load on fatigue life of bolted joints. However bolt load is limited to bolt axial strength in particular in the aeronautic field where bolts, mostly working in shear, have low axial strength for mass gain purpose.

The second way to increase friction load is to increase friction coefficient at joint interface. The proposed solution evaluated in this work is based on this method and uses friction shims industrialized by 3M. This technology is already used in the industry mainly to increase torque transfer in rotating systems (automotive, energy...) or to delete unwanted macro or micro sleeping

This study aims to identify and quantify the effect of technology that can increase friction when located at the interface of a titanium bolted joint. It considers the mechanical behaviour as well as the static and fatigue strengths. To the author's knowledge it is the first time that friction shims are studied to evaluate their impact on static and fatigue strength of aeronautics bolted joints. A finite element (FE) analysis will be developed to increase the understanding of phenomena at play in this study and to evaluate the best way to model them.

2 Specimen preparation and testing procedure

2.1 Test specimens

For the experimental test campaign, the specimens were single-lap bolted joints made of titanium (TA6V) plates. Table 1 and Figure 1 give the dimensions of specimens, all dimensions being computed from the nominal bolt diameter ($d=6.35\text{mm}$). The real bolt diameter was 6.33mm. \tilde{d} corresponded to the real hole diameter depending on the configuration. Fatigue and static specimens had different widths. For static loading specimens, a width of $W=7d$ was used to insure bolt-bearing failure, while a width of $W=4d$ was used for fatigue tests.

In the frame of hole-to-hole, three different configurations were used for the specimen geometry. Configurations A and B had aligned bolt holes with diameters of 6.38 and 6.88mm, respectively, while configuration C presented hole location errors in the loading direction, with opposite values of -0.5 and 0.5mm, and the diameter of the holes was 6.88mm. Table 2 presents the three different configurations and their associated clearances.

Table 1. Specimen geometry calculation and values

	d	\tilde{d}	a	L	e	p	W	t	
Calculation	-	-		$18d+a$	$2d$	$4d$	$\frac{7d}{2}$ (static)	$\frac{4d}{2}$ (fatigue)	$d/2$
Value (mm)	6.35	6.38 (A), 6.88 (B, C)	70	184.3	12.7	25.4	44.45	25.4	3.175

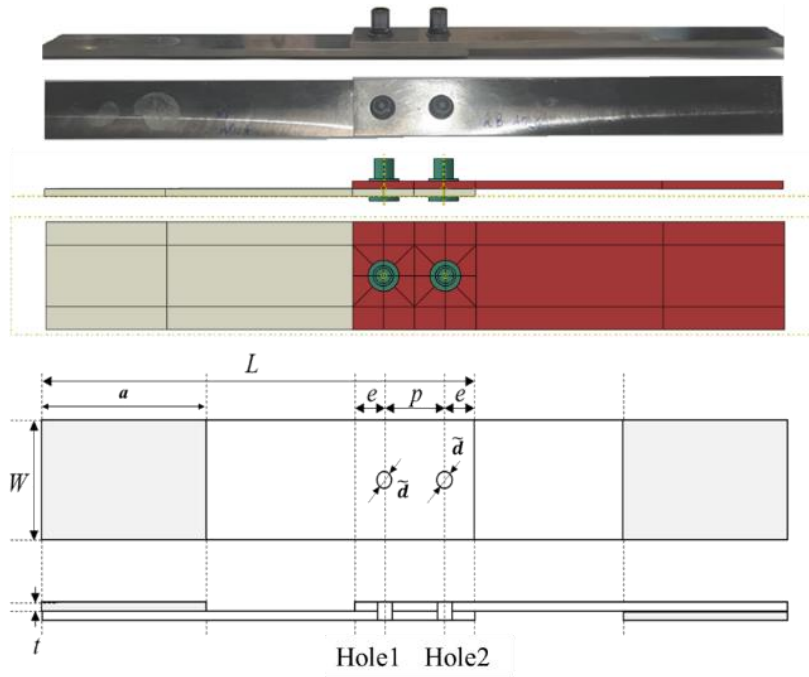



**Fig. 1.** Specimen geometry definition, numerical model and in reality

2.2 Friction washer

In this work, 3M industrial friction shims were used. Their geometry, positioning within the joint, and composition are given in Figure 2. A shim comprises a stack of three layers with a sheet of steel as the principal layer at the centre of the shim (0.15mm from micro measurement). On the exterior face, a thin layer of nickel is used to encapsulate diamonds. When the fasteners are installed, the diamonds create indentations in the specimen plates, thus creating higher friction grip. In this study grade 25 shims were used. The grade is based on the diamond average size, here 25 μ m. The shim has the shape of a washer with an inner diameter of 6.4mm and exterior diameter of 11mm.

Corrosion risk are not a major concern at this step of the study. Furthermore titanium is subject to corrosion, but the oxide layer formed becomes very protective and waterproof and its thickness slowly increases.

Table 2. Configurations tested with clearance, misalignment and geometry

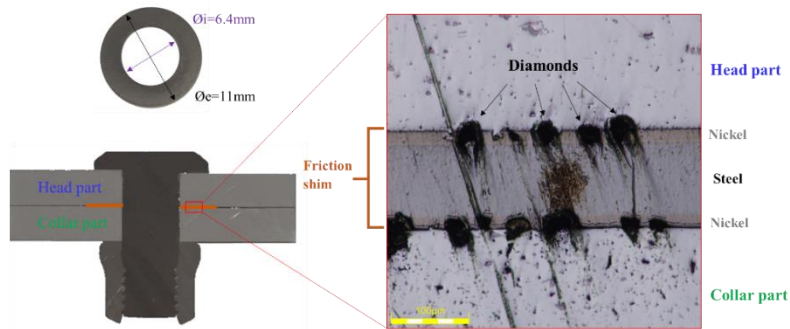
Configuration	Clearance (mm)	Misalignments (mm)	Geometry
A	0.05	0	
B	0.55	0	
C	0.55	0,5	

2.3 Testing setup

In this study, tensile tests to failure and fatigue tests were carried out to determine the joint behaviour in static and fatigue strength.

Firstly, the tensile tests aimed at determining the static ultimate strength of the joint. It was evaluated by applying a constant displacement of 0.5mm/min at the tip of the specimen up to failure. The results were used to identify the stress range for the following fatigue tests and correlate the FE model in Section 4. Finally, the tensile tests were also used to assess the critical slipping load, characterized by a strong relative displacement between the two plates of the joint (so called macro slipping).

The fatigue tests were carried out with a loading ratio of $R = \sigma_{\min} / \sigma_{\max} = 0.1$ and a frequency of 10 Hz. Each configuration was tested on seven specimens and the remote stresses applied were chosen to characterize the fatigue strength of the joints in the range of 10^4 to 10^6 cycles of fatigue life. The observed test results gave S-N curves and the Airbus Fatigue Indicator (AFI), corresponding to the stress level to reach a lifetime of 10^5 cycles.

**Fig. 2.** Friction shim positioning and composition from micro cut observations

3 Experimental test results and discussion

3.1 Static loading to failure

The static test results are gathered together in Figure 3. Those for configurations without friction shims are shown in dashed lines (A, B and C). The configurations with friction shims have solid lines (A_FS, B_FS and C_FS). The same nomenclature will be used for fatigue test results later in this paper. For reasons of confidentiality, the load has been normalized with the maximum ultimate load reached by configuration A_FS.

Joints without friction shim

At the beginning of the loading, all configurations follow the same path. In this phase, load is transmitted only by friction at the joint interface. Then, at a similar normalized load of 0.12, a change in curve slope can be observed for each specimen. The configurations A and C have a change of slope but the curve remains linear. However configuration B presents a nonlinear phase from 0.12 to 0.25 where the slope decreases then increases to finally become linear again with a slope similar to that of configuration A. This non-linear phase corresponds to macro-slipping. Theoretically, equation (1), can be used to compute the Coulomb's law friction coefficient, with F_N the normal load, which is the bolt load, F_T the tangential load and μ the friction coefficient. However, in this case, the macro slipping does not occur at a constant load level so it is hard to assess the correct tangential load. Assuming a friction coefficient of 0.4 for titanium/titanium contact [10] and knowing the normal load from previous instrumented installation tests, equation (1) gives a tangential normalized load value of 0.19. This value is in the middle of the macro-slipping zone and thus appears coherent.

$$F_T = \mu \cdot F_N \quad (1)$$

It can be observed that this phase only exists for configuration B. For configurations A and C, the transition between the two linear phases is almost direct due to the geometry and clearance parameters of those configurations.

After the macro-slipping, the shank of fasteners and the holes come into contact and the load is then transmitted through the fasteners by bearing. This phase is linear while the deformation within the plate and the bolts remain elastic. This elastic deformation lasts until around 0.69 for configurations A and B. Finally, a nonlinear phase begins and lasts up to final failure of the specimens – in this case by simultaneous shearing of the fasteners at a similar load of around 0.97.

For configuration C, the linear loading phase lasts until 0.46, when a nonlinear phase begins and continues until failure of the first fastener at 0.6 (fastener 2 in the scheme from Table 2.). At the instant of failure, the load drops from 0.6 to 0.29, then increases again until the final failure of the second bolt occurs at around 0.48.

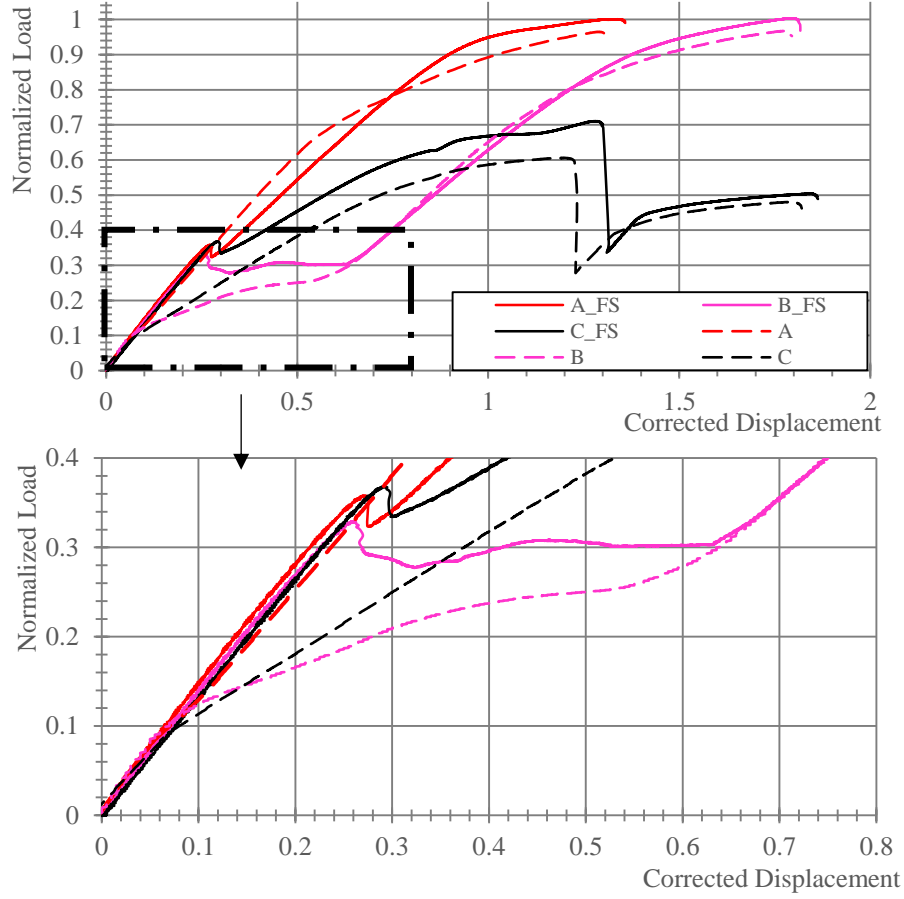


Fig. 3. Normalized load vs. global displacement during static tests and zoom on the early loading phases

Joints with friction shims

The global behaviour is very close to that without friction shims. The observed differences are described below.

The first linear phase, where load is transmitted by friction, reaches a much higher load: around 0.36 for configurations A and C, and 0.32 for configuration B.

After the slipping points for all the configurations, a small decrease of load, around 0.02, can be observed. This observation tends to indicate that the slipping behaviour of joints with friction shims has a static and a dynamic friction coefficient [11].

The macro-slipping phase is only visible on configuration B, similarly to a test without friction shim. However, it occurs at a quasi-constant load value of 0.30. Assuming the same bolt load, equation 1 gives values of 0.66 and 0.62 for the static and dynamic friction coefficients, respectively.

Regarding the elastic deformation phase of the fasteners, the yield strength seems to be higher for joints with friction shims. However, the final failure reaches a similar load level of 1.00 for configurations A and B.

For configuration C, the maximal load reached before failure, occurs at the same moment, just before failure of the first bolt. However, the load level is higher for joints with friction shims, as it reaches 0.71.

3.2 Fatigue tests

Figure 4 presents the fatigue test results and the S-N curves extrapolated from raw data. For reasons of confidentiality, stress data have been normalized so that the Airbus Fatigue Indicator (AFI) of the configuration A is set to 1. The AFI corresponds to the stress value for a fatigue life of 10^5 cycles.

The results show two distinct phenomena. Firstly, at high stress levels, the more impacting parameter is the geometric configuration. As expected, configuration A shows the highest fatigue life; for a normalized stress of 1.40, its fatigue life is around 40000 cycles. Configuration B follows, with a very similar fatigue life. Finally configuration C shows the worst fatigue life, with 25000 cycles.

Secondly, at low levels of stress, the more impacting parameter is the presence or absence of the friction shim. The highest numbers of cycles reached before failure were observed at a representative stress value around 0.88 for the three configurations with friction shims. For the three configurations without friction shims, the highest number of cycles reached before failure were observed at representative stress values around 0.7.

Finally, the three configurations with friction shims showed a 20% increase in their respective AFI compared with joints without friction shims. In particular, the AFI of configuration C_FS, despite the misalignment defects, was greater than the AFI from configuration A, representative of a conventional aeronautic joint.

3.3 Fatigue failure analysis

In this study, the design of specimens is such that failure occurs in the plates section close to the bolt holes. Due to the presence of two fasteners, the failure can occur on either the head part (hole 1), or the collar part (hole 2) as shown in Figure 5.

The failure location for each configuration is detailed in Table 3. It appears that the friction shim has no impact on the location on the failure. However, the geometric configuration tends to have an impact. For configuration A, the failure is equally distributed between the two sites; for configuration B, the failure occurs more often on the collar part; and for configuration C, the failure always occurs on the collar part.

After observing the failure locations, fracture profiles were observed. In all cases, with or without friction shim, the fatigue failure started at the joint interface as shown in Figure 6. From those observations it can be noted that friction shims have no impact on the failure profile, despite the increased friction at the interface.

Figure 6 also shows the gap between the two titanium plates when a friction shim is installed at the interface of the joint.

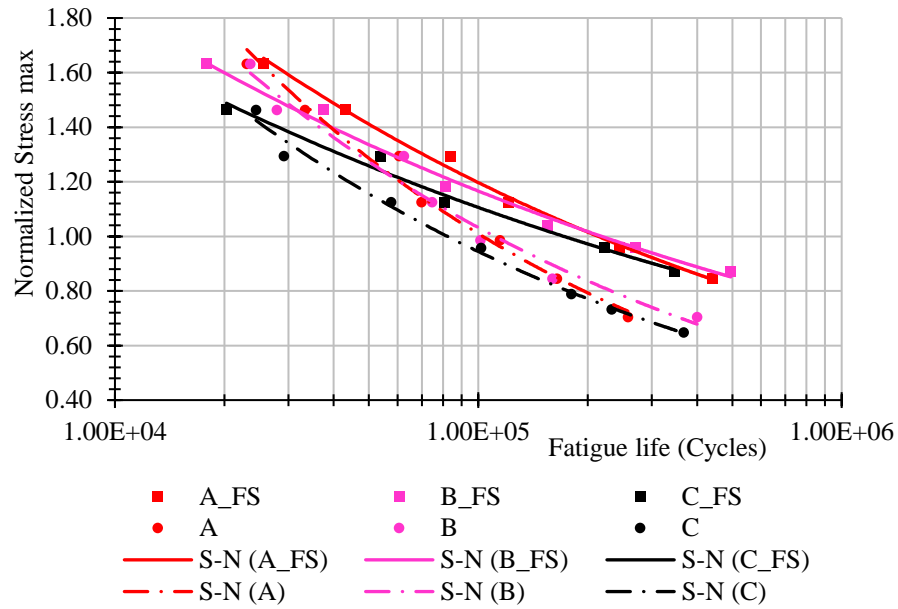


Fig. 4. Fatigue test results and associated S-N curves



Fig. 5. Fatigue failure locations, head side on the upper picture, collar side on the lower picture

Table 3. Fatigue failure side summary

Configuration	Number of failures on head part (hole 1)	Number of failures on collar part (hole 2)
A	4	3
B	1	6
C	0	7
A_FS	3	4
B_FS	2	5
C_FS	0	7

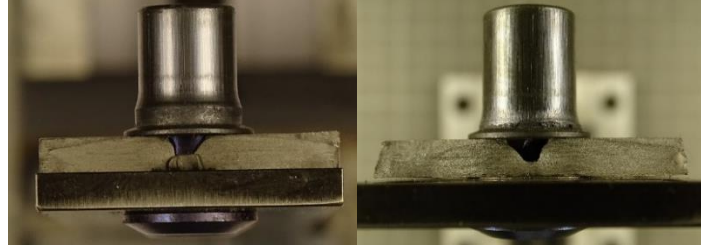


Fig. 6. Failure profiles for joints without friction shim on the left, with friction shim on the right

4 Finite Element analysis

To fully understand the observed experimental test results, a three-dimensional (3D) FE model was set up with the commercial code Abaqus[®]. The geometrical, material, and stress parameters were respected according to their description in Section 2. Materials were defined with their elastic-plastic behaviour. The parameters remain confidential. The model has three calculation steps. During the first step, the bolts are loaded under tension, and both plates are clamped at their extremity with no displacement allowed. The second step is a step of relaxation. The last step is the loading step. Plate 1 (head side) is clamped at its extremity while a ramp of displacement is imposed at the extremity of plate 2 (collar side). The value of the displacements corresponds to the ones observed experimentally up to failure of the bolts, or to the failure of the first bolt for configurations C and C_FS.

Contact is modelled with both a normal hard contact law and a tangential penalty law, for all the contact zone: bolt head/plate, collar/plate, bolt shank/plate, and plate/plate. A parametric study was run on the value of the penalty coefficient to match the experimental results. The final value of the penalty coefficient is 0.25 for configurations without friction shim. This value is lower than the one found experimentally, 0.4, but it is in agreement with previous results from McCarthy et al. [12].

There were some convergence difficulties with configuration B. The large macro slipping due to the large clearance generated some computation errors. To stabilize the contact, the elastic slip of the tangential law was increased from 0.005 to 0.01.

To model the configurations with friction shim, the plate/plate contact region was decreased to match the surface area of the washers. In addition, the friction coefficient was strongly increased to 0.7, once again following a parametric study. The bolt loads remained unchanged as the same bolts were used in all of the configurations.

Figure 9 presents the experimental and numerical load versus displacement curves. It can be observed that experimental and numerical results look very similar. The slight difference between A_FS and A_FS_NUM is due to the presence of clearance (0.06 mm) that was not taken into account in the numerical model. In the FE model, each contact load, normal or tangential, can be extracted. It was used to investigate the load distribution between fasteners and friction. In Figure 8, the evolution of each load: Bolt

1, Bolt 2 and Friction (with and without Friction Shim), is compared with the global load applied to the specimen for configurations C and C_FS. It can be observed that bolt 1 never transfers load. Static tests and numerical simulations have shown that failure of bolt 2 occurs before the contact of the first fastener, see Figure 7. These observations are coherent with the observed fatigue failure locations, as all failures were observed on hole number 2.

It can also be seen that the load carried by friction at the interface reaches a much higher maximum level for C_FS (0.28) than with C (0.1). Numerical results also show that the load transmitted by bolt 2 is higher by a value of 0.2 when the joint has no friction shims. Those observations are consistent with the experimental results.

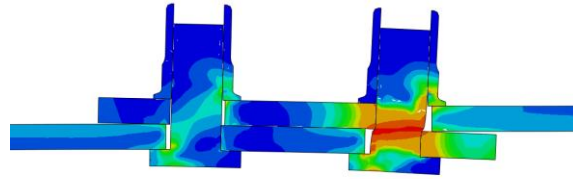


Fig. 7. Cut view of configuration C, under quasi-static loading at failure of bolt 2, Von Mises equivalent stress with deformation coefficient of 1

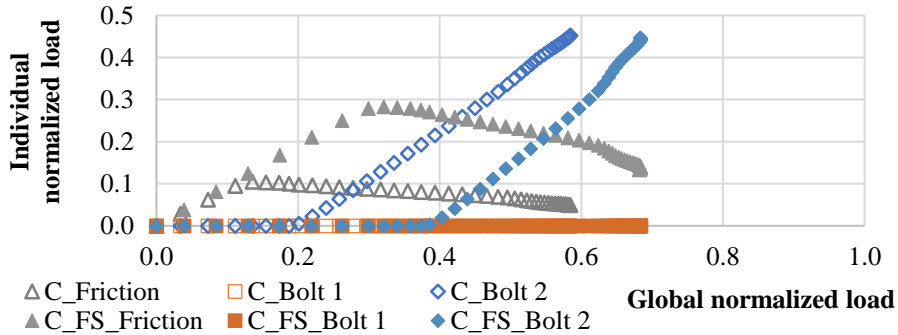


Fig. 8. Comparison between experimental and numerical results for configurations C without friction shims, and C_FS with friction shims

5 Conclusions

In this study, an experimental campaign was conducted to investigate the effect of 3M friction shims at the interface of titanium bolted joints. The criteria studied were mechanical behaviour, quasi-static strength and fatigue life. A 3D numerical model by FE was developed to investigate the phenomena involved in greater depth.

Regarding the mechanical behaviour, the experimental tests showed that the macro slipping occurred at higher loads for joints with friction shims, and that the slipping behaviour was a combination of static and dynamic friction. Despite convergence

difficulties, it was possible to obtain similar results numerically by strongly increasing the friction coefficient and reducing the elastic slip.

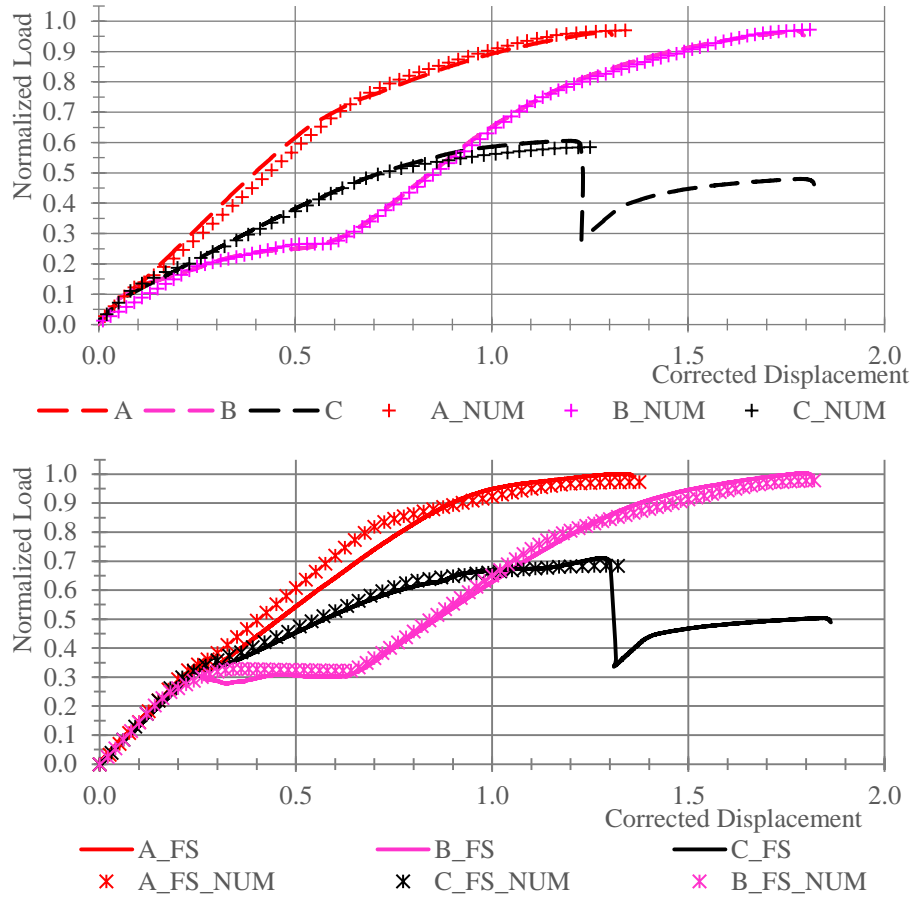


Fig. 9. Comparison between experimental and numerical results for configurations without friction shim on top and with friction shim on the bottom

Regarding static strength, friction shims have no impact on joints with aligned holes and have a low impact on joints with misaligned holes. The numerical model showed that, as the load increases in the bolts, the friction load decreases, explaining the observed results. In particular, for the configurations with misaligned holes, the heterogeneous distribution of load among the fasteners generated damage initiation in one of the bolts. The remaining one was not damaged, thus keeping the friction load effective.

Finally, regarding fatigue life, friction shims led to an increase of 20% on the Airbus Fatigue Indicator, even for joints with geometrical defects. The numerical model

showed that, at the same loading level, the joints with friction shims were transmitting less load through the bearing of the bolts, thus reducing the stress in the plates.

The next steps on this project are to run similar experiments with different plate material in particular aluminium and composite material widely use in the aeronautic industry. Corrosions risks will also be evaluated more intensively reading aluminium as this material is more sensitive to corrosion than titanium.

References

1. Bloem, J.: Developments in Hole-to-Hole Assembly. SAE Transactions, 116, 1087–1097 (2007).
2. Askri, R., Bois, C., Wagnier, H.: Effect of Hole-location Error on the Strength of Fastened Multi-Material Joints. *Procedia CIRP*, 43, 292-296 (2016).
3. Lecomte, J., Bois, C., Wagnier, H., Wahl, J.-C.: An analytical model for the prediction of load distribution in multi-bolt composite joints including hole-location errors. *Composite Structures*, 117, 354-361 (2014).
4. Liu, F., Shan, M., Zhao, L., Zhang, J.: Probabilistic bolt load distribution analysis of composite single-lap multi-bolt joints considering random bolt-hole clearances and tightening torques. *Composite Structures*, 194, 12-20 (2018).
5. McCarthy, M.A., Lawlor, V.P., Stanley, W.F., McCarthy C.T.: Bolt-hole clearance effects and strength criteria in single-bolt, single-lap composite bolted joints, *Composites Science and Technology*, 62 (10–11), 1415-1431 (2002).
6. Lawlor, V.P., McCarthy, M.A., Stanley, W.F.: An experimental study of bolt–hole clearance effects in double-lap, multi-bolt composite joints. *Composite Structures*, 71, Issue 2, 176-190 (2005).
7. Benhaddou, T., Stephan, P., Daidié, A., Alkatan, F., Chirol, C., Tuery, J.B.: Effect of axial preload on durability of aerospace fastened joints. *International Journal of Mechanical Sciences*, 137, 214-223 (2018).
8. McCarthy, C.T., Gray, P.J.: An analytical model for the prediction of load distribution in highly torqued multi-bolt composite joints. *Composite Structures*, 93, Issue 2, 287-298 (2011).
9. 3M Friction Shims gasket (PDF):
<https://multimedia.3m.com/mws/media/1722448O/crrc3m-friction-shims-friction-gasket.pdf>
10. Meier, L., Schaal, N., Wegener, K.: In-process Measurement of the Coefficient of Friction on Titanium. *Procedia CIRP*, 58, 163-168 (2017).
11. Berardo, A., Costagliola, G., Ghio, S., Boscardin, M., Bosia, F., Pugno, N. M.: An experimental-numerical study of the adhesive static and dynamic friction of micro-patterned soft polymer surfaces. *Materials & Design*, 181, 107930 (2019).
12. McCarthy, C.T., McCarthy, M.A., Stanley, W.F., Lawlor, V.P.: Experiences with Modeling Friction in Composite Bolted Joints. *Journal of Composite Materials*, 39, 1881-1908 (2005).